

Fabrication and Photocatalytic Properties of TiO₂ Nanotube Arrays Modified with Phosphate

Kazuya Nakata,^{*1,2,3} Baoshun Liu,¹ Yosuke Ishikawa,^{1,4} Munetoshi Sakai,^{1,2} Hidenori Saito,² Tsuyoshi Ochiai,^{1,3} Hideki Sakai,⁴ Taketoshi Murakami,¹ Masahiko Abe,^{3,4} Katsuhiko Takagi,² and Akira Fujishima^{*1,2,3}

¹Photocatalyst Group, Kanagawa Academy of Science and Technology,

KSP Building East 412, 3-2-1 Sakado, Takatsu-ku, Kawasaki, Kanagawa 213-0012

²Organic Solar Cell Assessment Project, Kanagawa Academy of Science and Technology,

KSP Building East 308, 3-2-1 Sakado, Takatsu-ku, Kawasaki, Kanagawa 213-0012

³Research Institute for Science and Technology, Energy and Environment Photocatalyst Research Division, Tokyo University of Science, 1-3 Kagurazaka, Shinjuku-ku, Tokyo 162-8601

⁴Faculty of Science and Technology, Tokyo University of Science, 2641 Yamazaki, Noda, Chiba 278-8510

(Received June 29, 2011; CL-110548; E-mail: pg-nakata@newkast.or.jp)

We have prepared TiO₂ nanotubes by anodization in HF or HF/H₃PO₄ mixed electrolyte. The morphologies and photocatalytic properties of the nanotubes were changed by electrolytes. The nanotubes prepared in HF/H₃PO₄ mixed electrolyte showed higher performance to decompose acetaldehyde by photocatalysis than those prepared in pure HF.

Titanium dioxide (TiO₂) has been widely studied since the discovery of photoelectrochemical water splitting by Fujishima and Honda¹ because it shows a strong oxidation ability that can be used not only for water splitting but also many other practical applications.^{2–4} For example, TiO₂ coatings applied to glass and ceramic substrates can provide a self-cleaning surface that removes organic contaminants. For this purpose, TiO₂ surfaces that exhibit high performance for the photocatalytic degradation of organic compounds are being investigated by many researchers. Anodized TiO₂ nanotube arrays^{5,6} are a potential candidate for this role because they can photocatalytically degrade organic compounds efficiently. This is a result of their large effective surface area, straight channels that enable diffusion of oxidizable species into the TiO₂ nanotubes, and less recombination because the thickness of half of the nanotube wall is significantly less than the carrier diffusion length in TiO₂.⁷ The photocatalytic performance of TiO₂ nanotubes depends on morphology, especially their length.⁵ When the length of a nanotube increases, its surface area increases, which leads to high photocatalytic performance. However, longer TiO₂ nanotubes tend to break easily and separate from the substrate.⁸ Another method to increase photocatalytic performance is surface modification with nonmetal atoms (N, S, C, B, P, and F)^{9–15} or anion molecules.^{16–19} For example, Zhao et al. reported that surface modification of TiO₂ powders with phosphate-improved photocatalytic performance.¹⁶ Such surface modification should increase electron–hole separation, which in turn influences photocatalytic performance.

In this work, to obtain photocatalysts that exhibit high performance, TiO₂ nanotubes modified with phosphate are prepared by anodization in a mixed electrolyte containing hydrofluoric acid (HF) and phosphoric acid (H₃PO₄). The structures, crystal phases, and photocatalytic properties of the resulting materials are investigated.

Highly ordered TiO₂ nanotube arrays were prepared by potentiostatic anodization in a two-electrode electrochemical

cell. Titanium foil (0.25 mm thick, 5 × 3 cm) was used as the working electrode, and platinum foil (5 × 1 cm) served as the counter electrode. The distance between the working and counter electrodes was 1 cm. A voltage was applied with a DC power supply (E3612A, Agilent Technologies). Anodization was performed in three different electrolytes (30 mL) consisting of 0.5 vol % HF for sample 1, 0.5 vol % HF and 1 M H₃PO₄ for sample 2, and 0.5 vol % HF and 4 M H₃PO₄ for sample 3 at 25 V for 1 h at room temperature. After anodization, the Ti foils were removed from solution under continued application of potential and washed with Milli-Q water. The films were calcined at 500 °C under atmospheric conditions for 3 h.

Cross-sectional and top view images of TiO₂ nanotube arrays prepared in different electrolytes are shown in Figure 1. To prepare the TiO₂ nanotubes in sample 1, titanium foil was anodized in an electrolyte containing 0.5 vol % HF at 25 V for 1 h, resulting in the formation of a TiO₂ nanotube array containing nanotubes with a length of about 160 nm, inner diameter of about 95 nm, and wall thickness of about 6 nm (Figure 1a). A cross-sectional image of sample 1 revealed that this TiO₂ nanotube array is highly ordered and oriented perpendicular to the titanium substrate. To produce sample 2 (Figure 1b), titanium foil was anodized in a mixed electrolyte containing both HF and H₃PO₄. A regular, well-aligned nanotube array containing nanotubes with a length of about 505 nm, average inner diameter of about 96 nm, and wall thickness of about 8 nm was obtained. When a mixed electrolyte with a high concentration of H₃PO₄ was used (sample 3, Figure 1c), the

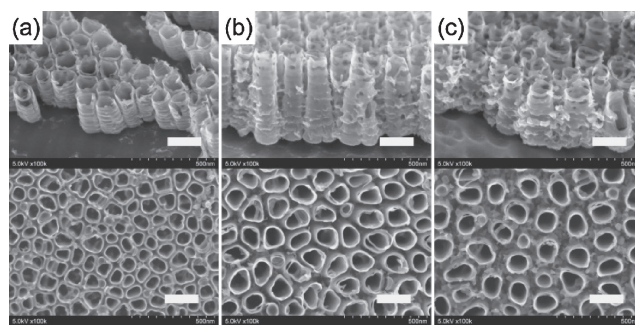


Figure 1. Cross-sectional and top view images of TiO₂ nanotube arrays prepared in different electrolytes. Sample (a) 1, (b) 2, and (c) 3. Scale bar is 200 nm.

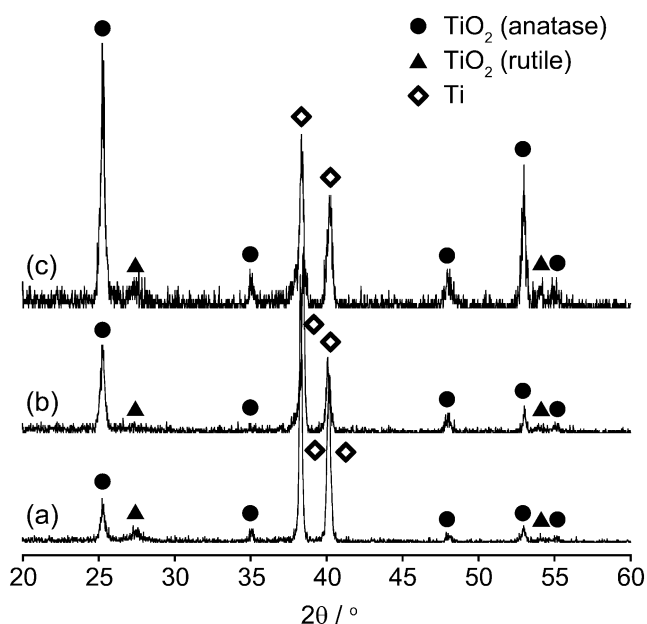


Figure 2. X-ray diffraction patterns of TiO₂ nanotube array samples (a) 1, (b) 2, and (c) 3.

obtained TiO₂ nanotubes had a length of about 309 nm, average inner diameter of about 99 nm, and a wall thickness of about 11 nm. These results suggest that the presence of H₃PO₄ affects the morphology of TiO₂ nanotubes, causing a significant increase in length, slight increase in diameter, and wall thickness compared with using pure HF. Generally, the formation of TiO₂ nanotube arrays in a fluoride-based electrolyte results from two main factors: electrochemical oxidation and chemical dissolution.^{20,21} The rate of chemical dissolution of TiO₂ by fluoride ions is strongly related to the concentration of H⁺ ions in the electrolyte and influences the morphology of the nanotube arrays. The observed changes in morphology may be caused by H₃PO₄ behaving as a pH buffer, which is a factor that is known to affect pore geometry and helps to regulate local acidification during pore growth as has been discussed in detail previously.²²

XRD patterns of the TiO₂ nanotube arrays prepared by anodization in different electrolytes after annealing at 500 °C under atmospheric conditions for 3 h are presented in Figure 2. The pattern of sample 1 has peaks consistent with the anatase phase at $2\theta = 25.2, 35.1, 47.8, 52.9,$ and 55.1° that can be indexed to the (101), (103), (200), (105), and (211) crystal faces of anatase TiO₂, respectively. This sample also contains some TiO₂ in the rutile phase, with peaks at $2\theta = 27.6$ and 54.0° that can be indexed to the (110) and (211) crystal faces of rutile TiO₂, respectively. Samples 2 and 3 also contained a mixture of anatase and rutile TiO₂. It seems that sample 3 has better crystallinity, which can lead to better photocatalytic performance (see below).

The photocatalytic properties of the calcined TiO₂ nanotubes were investigated by studying their ability to photocatalytically decompose acetaldehyde and simultaneously produce CO₂ under UV irradiation, as shown in Figure 3. After equilibration in the dark for 2 h, the concentration of acetaldehyde decreased from 300 to 224 ppm in nanotube sample 1, which was caused by the physical adsorption of acetaldehyde on

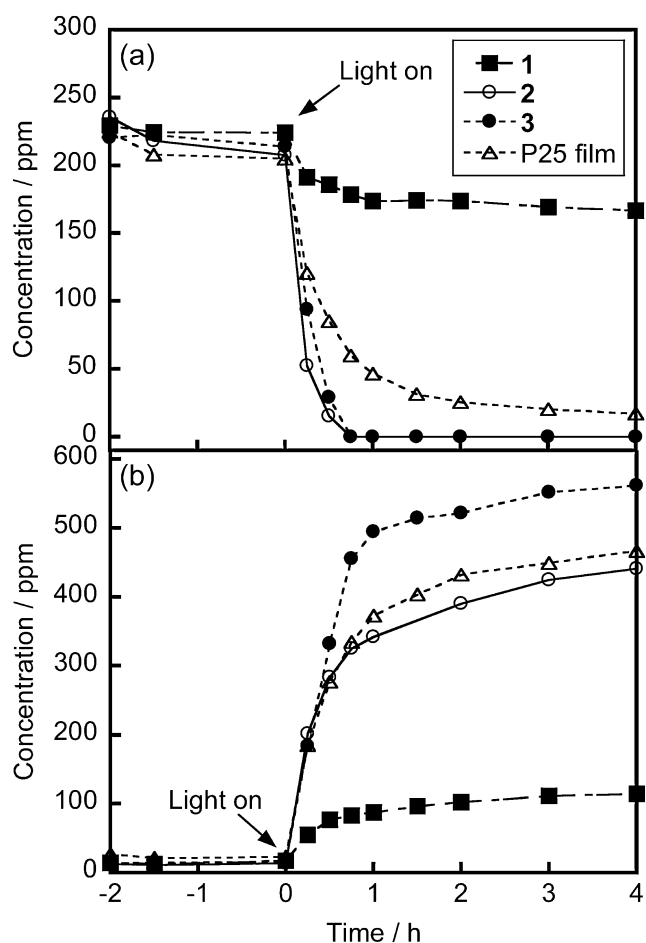


Figure 3. (a) Photocatalytic decomposition of acetaldehyde and (b) simultaneous generation of CO₂ by TiO₂ nanotube array samples 1–3 and P25 film under UV irradiation.

the surface of the nanotubes. Upon irradiation with UV light with an intensity of 1 mW cm^{-2} , the concentration of acetaldehyde decreased slightly, and the concentration of CO₂ increased to 114 ppm after 4 h. In contrast, in samples 2 and 3, the concentration of acetaldehyde decreased significantly, and simultaneous CO₂ generation increased substantially to 441 and 562 ppm, respectively, under irradiation with UV light. From the above results, the rates of acetaldehyde decomposition and CO₂ generation by samples 2 and 3 are faster than that by sample 1. The nanotubes in samples 2 and 3 are longer than those in sample 1, so the surface area is larger in samples 2 and 3, which may increase their photocatalytic performance. However, the nanotubes in samples 2 and 3 are almost the same length, but the photocatalytic performance of sample 3 is higher than that of sample 2. This indicates that the photocatalytic performance of the nanotube arrays is not only controlled by surface area. Another factor is crystallinity. For reference, a particulate film consisting of P25 particles (Degussa) with a thickness of about 500 nm was prepared and photocatalytic performance evaluated (preparation and cross-sectional images of the P25 film are provided in Supporting Information).^{6,23} P25 powders have high crystallinity and show high photocatalytic performance for degradation of acetaldehyde. Nevertheless,

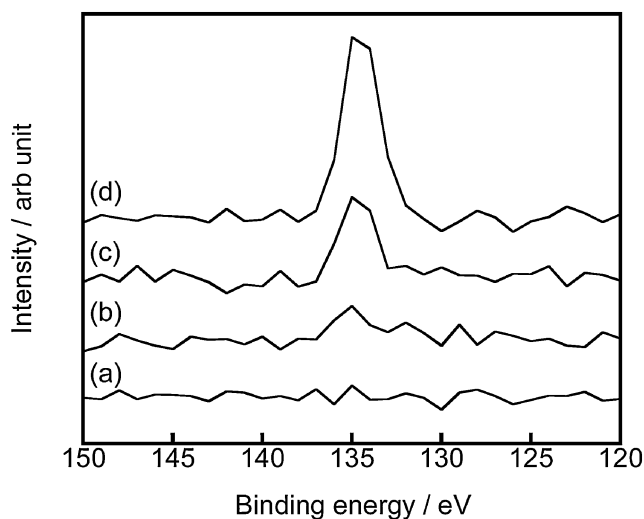


Figure 4. XPS spectra of the P 2p peak on the surface of samples (a) **1**, (b) **2** after etching to a depth of 30 nm, (c) **2**, and (d) **3**.

sample **3** shows superiority for photocatalytic degradation of acetaldehyde and generation of CO_2 than that of the P25 film, which indicates that factors affecting photocatalytic performance may not be only the crystallinity. Furthermore, this is comparable with long TiO_2 nanotubes reported in a previous paper. The long nanotube of $8.4 \mu\text{m}$ has better photocatalytic performance than that of the P25 film. In contrast, the short nanotube of **3** modified with phosphate has also better photocatalytic performance than that of the P25 film. The high photocatalytic performance for sample **3** should be due to not only surface area and crystallinity but also the presence of PO_4^{3-} ions (see below).

The presence of PO_4^{3-} ions should also affect the photocatalytic properties of the nanotube arrays. Figure 4 shows XPS spectra of the TiO_2 nanotube arrays prepared in different electrolytes. The spectrum of sample **1** indicates that P species are not present, whereas the spectra of samples **2** and **3** contain a peak at around 135 eV that is consistent with PO_4^{3-} ions. These results suggest that PO_4^{3-} ions are adsorbed on the TiO_2 nanotubes during anodization in $\text{HF}/\text{H}_3\text{PO}_4$ mixed electrolytes. After the surface of sample **2** was etched to a depth of 30 nm, the intensity of the signal around 135 eV decreased, indicating that PO_4^{3-} is only present close to the surface of the nanotubes. In the case of samples **2** and **3**, PO_4^{3-} will promote the separation of holes and electrons, which may affect the photocatalytic properties of these nanotube arrays.^{16,19} Note that the contents of P on sample **2** and **3** are 2.4% and 4.2%, which increase with the concentration of electrolytes when prepared.

In summary, TiO_2 nanotubes were prepared by anodization in HF or $\text{HF}/\text{H}_3\text{PO}_4$ mixed electrolyte. The morphology of the resulting TiO_2 nanotubes is significantly influenced by the electrolyte. The length, diameter, and wall thickness of the TiO_2 nanotubes increased upon addition of H_3PO_4 . XRD measure-

ments revealed that the TiO_2 nanotubes are mostly anatase but also contain some of the rutile phase. The photocatalytic performance of the arrays was evaluated by their ability to decompose acetaldehyde and simultaneously generate CO_2 . The nanotubes prepared in $\text{HF}/\text{H}_3\text{PO}_4$ mixed electrolyte showed higher performance than those prepared in pure HF . Crystallinity and the presence of PO_4^{3-} ions on the surfaces of the samples prepared in $\text{HF}/\text{H}_3\text{PO}_4$ mixed electrolyte should affect their photocatalytic properties.

References and Notes

- 1 A. Fujishima, K. Honda, *Nature* **1972**, *238*, 37.
- 2 A. Fujishima, K. Hashimoto, T. Watanabe, *TiO₂ Photocatalysis: Fundamentals and Applications*, BKC, **1999**.
- 3 A. Fujishima, T. N. Rao, D. A. Tryk, *J. Photochem. Photobiol., C* **2000**, *1*, 1.
- 4 A. Fujishima, X. Zhang, D. A. Tryk, *Surf. Sci. Rep.* **2008**, *63*, 515.
- 5 Z. Liu, X. Zhang, S. Nishimoto, T. Murakami, A. Fujishima, *Environ. Sci. Technol.* **2008**, *42*, 8547.
- 6 Z. Liu, X. Zhang, S. Nishimoto, M. Jin, D. A. Tryk, T. Murakami, A. Fujishima, *J. Phys. Chem. C* **2008**, *112*, 253.
- 7 C. A. Grimes, G. K. Mor, *TiO₂ Nanotube Arrays: Synthesis, Properties and Applications*, Springer, **2010**.
- 8 J. Wang, Z. Lin, *Chem. Mater.* **2008**, *20*, 1257.
- 9 R. Asahi, T. Morikawa, T. Ohwaki, K. Aoki, Y. Taga, *Science* **2001**, *293*, 269.
- 10 T. Ihara, M. Miyoshi, Y. Iriyama, O. Matsumoto, S. Sugihara, *Appl. Catal., B* **2003**, *42*, 403.
- 11 S. U. M. Khan, M. Al-Shahry, W. B. Ingler, Jr., *Science* **2002**, *297*, 2243.
- 12 T. Tachikawa, S. Tojo, K. Kawai, M. Endo, M. Fujitsuka, T. Ohno, K. Nishijima, Z. Miyamoto, T. Majima, *J. Phys. Chem. B* **2004**, *108*, 19299.
- 13 W. Zhao, W. Ma, C. Chen, J. Zhao, Z. Shuai, *J. Am. Chem. Soc.* **2004**, *126*, 4782.
- 14 L. Lin, W. Lin, Y. Zhu, B. Zhao, Y. Xie, *Chem. Lett.* **2005**, *34*, 284.
- 15 D. Li, H. Haneda, S. Hishita, N. Ohashi, *Chem. Mater.* **2005**, *17*, 2596.
- 16 D. Zhao, C. Chen, Y. Wang, H. Ji, W. Ma, L. Zang, J. Zhao, *J. Phys. Chem. C* **2008**, *112*, 5993.
- 17 J. C. Yu, W. Ho, J. Yu, S. K. Hark, K. Iu, *Langmuir* **2003**, *19*, 3889.
- 18 L. Körösi, I. Dékány, *Colloids Surf., A* **2006**, *280*, 146.
- 19 L. Körösi, S. Papp, I. Bertóti, I. Dékány, *Chem. Mater.* **2007**, *19*, 4811.
- 20 J. M. Macák, H. Tsuchiya, P. Schmuki, *Angew. Chem., Int. Ed.* **2005**, *44*, 2100.
- 21 X. Feng, J. M. Macak, P. Schmuki, *Chem. Mater.* **2007**, *19*, 1534.
- 22 S. Bauer, S. Kleber, P. Schmuki, *Electrochem. Commun.* **2006**, *8*, 1321.
- 23 Supporting Information is available electronically on the CSJ-Journal Web site, <http://www.csj.jp/journals/chem-lett/index.html>.